Annular Hurricanes

JOHN A. KNAFF AND JAMES P. KOSSIN

Cooperative Institute for Research in the Atmosphere, Colorado State University, Fort Collins, Colorado

MARK DEMARIA

NOAA/NESDIS, Fort Collins, Colorado

(Manuscript received 15 January 2002, in final form 15 October 2002)

ABSTRACT

This study introduces and examines a symmetric category of tropical cyclone, which the authors call annular hurricanes. The structural characteristics and formation of this type of hurricane are examined and documented using satellite and aircraft reconnaissance data. The formation is shown to be systematic, resulting from what appears to be asymmetric mixing of eye and eyewall components of the storms involving either one or two possible mesovortices. Flight-level thermodynamic data support this contention, displaying uniform values of equivalent potential temperature in the eye, while the flight-level wind observations within annular hurricanes show evidence that mixing inside the radius of maximum wind likely continues. Intensity tendencies of annular hurricanes indicate that these storms maintain their intensities longer than the average hurricane, resulting in larger-than-average intensity forecast errors and thus a significant intensity forecasting challenge. In addition, these storms are found to exist in a specific set of environmental conditions, which are only found 3% and 0.8% of the time in the east Pacific and Atlantic tropical cyclone basins during 1989–99, respectively. With forecasting issues in mind, two methods of objectively identifying these storms are also developed and discussed.

1. Introduction

The satellite appearance of tropical cyclones can vary widely from case to case and from day to day. This study introduces a category of tropical cyclone, termed annular hurricanes. When compared with the greater population of tropical cyclones in an archive of infrared (IR) tropical cyclone imagery, these storms are distinctly more axisymmetric with circular eyes surrounded by a nearly uniform ring of deep convection and a curious lack of deep convective features outside this ring. Because of this symmetry, these storms have also been referred to as truck tires and doughnuts. This appearance in satellite imagery can persist for days. Accompanying this structure is a nearly constant intensity[1] with an average of 107.6 kt (1 kt = 0.514 m s^{-1}). This characteristic represents a potential source for large intensity forecasting errors, which may be reduced by better identification of annular hurricanes. For this reason, a comparison of the intensity evolution of annular hurricanes in the context of intensity forecasting will be examined in this paper.

The rather persistent structural appearance displayed in annular hurricanes suggests that there are special circumstances related to their formation and persistence. Based on modeling and theoretical studies (Jones 1995; Bender 1997; Frank and Ritchie 1999, 2001) environmental wind shear should be intimately related to the symmetry of these systems. Using environmental data, this paper will document the vertical shear and other environmental conditions that are associated with annular hurricane occurrences and how they differ from a large sample of tropical cyclones.

The lack of in situ wind and radar observations is an unfortunate reality that is common when studying tropical cyclones; however, animated IR satellite imagery combined with aircraft reconnaissance, when available, can be used to infer the dynamics and thermodynamics associated with annular hurricanes and their formation. This methodology will be pursued in the context of a number of recent studies (Schubert et al. 1999; Kossin et al. 2000; Montgomery et al. 2000; Kossin and Schubert 2001) that have considered the role that barotropic instability and asymmetric potential vorticity (PV) mixing processes might play in the region of the hurricane inner core. Using aircraft flight-level data from hurri-

[1] Because the maximum winds for tropical cyclones are forecast and archived (Davis et al. 1984; Jarvinen et al. 1984) in knots, knots are the units used for intensity throughout this paper.

Corresponding author address: John A. Knaff, NOAA Cooperative Institute for Research in the Atmosphere, Colorado State University, Fort Collins, CO 80523-1375.
E-mail: knaff@cira.colostate.edu

canes, Kossin and Eastin (2001) showed that radial profiles of vorticity and equivalent potential temperature (θ_e) often undergo rapid and dramatic changes from a barotropically unstable regime (i.e., $\partial^2 v/\partial r^2 > 0$ and $\partial\theta_e/\partial r > 0$), which they refer to as regime 1, to a barotropically stable regime (i.e., $\partial^2 v/\partial r^2 \leq 0$ and $\partial\theta_e/\partial r \cong 0$), or regime 2, and they hypothesized that these changes may result from horizontal mixing processes.

The current study concentrates upon six annular hurricanes that have been observed in the Atlantic (1995–99) and eastern North Pacific (1997–99) tropical cyclone basins. A factor in determining the number and location of storms investigated in this study is the availability of a tropical cyclone IR satellite dataset, which exists for 1995–2001 in the Atlantic and 1997–2001 in the eastern Pacific. Additionally, uniform measurements of environmental conditions calculated for the purpose of intensity forecasting are available from 1989 to 1999. We know that annular hurricane have occurred in other tropical cyclone basins; however, neither of these datasets is readably available in other tropical cyclone basins. It is the desire to perform quantitative analysis involving both the environmental conditions and the IR brightness temperatures that excludes annular hurricanes in other basins and earlier times from this study. In addition to the IR imagery and the environmental conditions, a variety of other datasets is also used to investigate these axisymmetric storms.

The structural and intensity characteristics of annular hurricanes suggest methods to objectively identify them may be both possible and useful. The identification of annular hurricanes, especially in a real-time forecast setting, may possibly be utilized to improve intensity estimations and forecasts. For this reason objective identification techniques, which use structural and environmental characteristics found during the course of this study, will also be explored.

To begin the examination of annular hurricanes, section 2 offers descriptions of the various datasets that are used in this study. Following this brief discussion of datasets, the features of annular hurricanes, including their axisymmetry, intensity characteristics and forecast errors, formation, and associated environmental conditions, will be shown in section 3. Using the evolutionary, structural, and environmental characteristics of these storms detailed in section 3, section 4 discusses the development of objective techniques to better identify these hurricanes in a real-time forecasting setting. The final section will present a summary of this study along with a few concluding remarks and relevant observations.

2. Datasets

Several datasets are used to study annular hurricanes. Half-hourly Geostationary Operational Environmental Satellite (GOES) images are used to examine cloud structures. These images have a 4-km horizontal resolution after being remapped to a Mercator projection. This IR dataset includes all storms for the period 1995–2001 in the Atlantic, and 1997–2001 in the eastern Pacific, for this reason in this study we concentrate on annular hurricanes that occurred after 1995. The dataset is part of a tropical cyclone IR image archive maintained at the National Oceanic and Atmospheric Administration's (NOAA) Cooperative Institute for Research in the Atmosphere (Zehr 2000).

The track and intensity of each storm come from digital databases of best-track information discussed in Davis et al. (1984) and Jarvinen et al. (1984), which are maintained at the National Hurricane Center (NHC). The Atlantic best-track dataset starts in 1870 and the east Pacific best-track dataset starts in 1945. Another dataset referred to as the extended Atlantic best-track dataset exists for the years 1988–2001 and contains additional storm-scale information including radii of significant (maximum, and 34, 50, and 64 kt) winds, and eye size. The extended Atlantic best-track data (DeMaria et al. 2001) are used to discuss structural differences between annular hurricanes and the Atlantic mean, since reliable estimates of these structural quantities, namely wind radii and eye size, often do not exist for other basins, where routine reconnaissance is unavailable. For these comparison purposes, eye sizes of annular hurricanes were estimated using the IR imagery.

To compare the life cycle of tropical cyclones with intensities greater than 64 kt with the life cycle of annular hurricanes, we rely upon the past work of Emanuel (2000) who showed that the life cycles of Atlantic hurricanes and west Pacific typhoons are remarkably similar. Unfortunately, Emanuel (2000) did not examine east Pacific hurricanes explicitly; however, the remarkable similarity between the intensity evolutions in these two quite different basins suggest, that the intensity evolution in the eastern Pacific is likely similar.

The rate at which tropical cyclones weaken is also of interest. To determine standard weakening rates, two methods are used: one from empirics and another from theory. The weakening of tropical cyclones is a fundamental aspect of the Dvorak method for tropical cyclone intensity analysis (Dvorak 1984). The rate of weakening is given in terms of *T* numbers, which are related to current intensities. The rules associated with this method limit the number of *T* numbers that is allowed to change in a 24-h period, which is a maximum filling rate. These same rules give guidelines for average and slower than average weakening rates. These empirically derived rates are compared to those created using the theory of Eliassen and Lystad (1977), which has been applied to tropical cyclones in Montgomery et al. (2001). In this theory vortex spindown is controlled by the toroidal circulations (u, w) forced by the Ekman layer, and offers a maximum weakening rate under the assumption that inertial toroidal oscillations are neglected.

Two sorties of flight-level data are available for ex-

amining annular hurricanes. These are the periods containing 0000 UTC 4 September 1995 for Hurricane Luis and 0600 UTC 15 August 1999 for Hurricane Dora. These aircraft reconnaissance data were collected by the Fifty-third Weather Reconnaissance Squadron and are available in a 10-s temporal resolution. Each sortie contained three transects of the storm.

Environmental conditions associated with annular hurricanes are obtained using the predictors calculated for the Statistical Hurricane Intensity Prediction Scheme (SHIPS), which are available at 12-h increments (DeMaria and Kaplan 1994a, 1999). The SHIPS atmospheric information is derived from National Centers for Environmental Prediction (NCEP) global model analyses through 1999. In this process the storm circulation is removed using a Laplacian filter, which performs a linear interpolation across a circular area encompassed by radius R and effectively removes the storm-scale circulation from the environmental flow. This filter is applied to the original model as described in DeMaria and Kaplan (1999) and the data were saved in a 2° latitude–longitude grid (2.5° prior to 1996). In this filtering process $R = 800$ km at 1000 hPa and decreases linearly to $R = 500$ km at 100 hPa. Once this filter has been applied to the analyses, which effectively removes the storm-scale circulation from the environmental flow, average environmental factors are calculated within 1000 km of the storm center, except for vertical wind shear, which is averaged within a distance of 600 km. Since the current formulation of SHIPS no longer uses the Laplacian filter to create area-average predictors, our analysis is limited to storms that formed prior to 1999.

Environmental factors calculated for the SHIPS model include temperature, zonal wind, relative eddy momentum flux convergence (REFC) and divergence at 200 hPa, vorticity at 850 hPa, and vertical wind shear between 200 and 850 hPa and 500 and 850 hPa. The REFC is calculated from

$$\text{REFC} = -r^{-2}\frac{\partial}{\partial r}(r^2\overline{U_L'V_L'}), \quad (1)$$

where r is the radius from storm center, U is the radial wind, V is the tangential wind, the overbar represents an azimuthal average with respect to the storm center, the primes represent deviations from that average, and the subscript L indicates a coordinate system moving with the storm. If not calculated in a motion-following coordinate, storm motion would result in a positive REFC. Point values of SST used by SHIPS are derived from weekly SST fields described in Reynolds and Smith (1994). Since the environments of tropical cyclones has been well examined in the literature we choose to use a combined Atlantic and east Pacific tropical cyclone climatology for the purposes of identifying the characteristic environments associated with the average annular hurricane. In doing so the authors recognize that some biases may be introduced into the results of this study.

The authors also recognize that the operational analyses carry with them a host of errors and uncertainties. However, as described in Molinari et al. (1992), these analyses possess sufficient quality to deduce large-scale environmental factors such as vertical wind shear and fluxes of angular momentum. Further proof of the usefulness of these analyses with respect to tropical cyclone studies comes from the ability of SHIPS to provide skillful hurricane intensity predictions using data derived from these analyses (DeMaria and Kaplan 1999).

3. Features of annular hurricanes

Before the features associated with annular hurricanes can be examined, annular hurricane cases must be identified. The IR imagery is the visual means by which we determine whether a storm is an annular hurricane. An annular hurricane is identified if the hurricane persists for at least 3 h in an axisymmetric state defined by the following: 1) the hurricane has a normal-to-large-sized circular eye surrounded by a single band of deep convection containing the inner-core region and 2) the hurricane has little or no convective activity beyond this annulus of convection. The use of digital IR data also allows for the development of an objective technique of identifying storms with these characteristics, which will be addressed in section 4. Note that a hurricane is considered an annular hurricane only when these conditions are met; before and after the annular phase, the hurricane is considered an asymmetric storm. The six hurricanes that meet these subjective criteria during our period of study are listed in Table 1 along with ranges of satellite estimates of the range of eye sizes and best-track-determined intensities. Further details on the characteristics of these storms are described in sections 4a–d.

a. Axisymmetry

The first feature that separates annular hurricanes from the general population of hurricanes is the degree of axisymmetry displayed in IR imagery. Figure 1 shows IR images of each of the annular hurricanes listed in Table 1. Many of the defining attributes of an annular hurricane are displayed in this figure. First, annular hurricanes have nearly circular eyes and these eyes have larger radii (see Table 1) than the Atlantic average of 23 km (sample size = 415, standard deviation = 5.3 km), as determined from the extended Atlantic best track for storms with intensities greater than 85 kt. The second feature that all annular hurricanes have is a nearly symmetric annulus of deep convection (IR brightness temperatures) surrounding the circular eye, although some small asymmetries in cloud-top temperature within this annulus still exist as shown in the enhanced images shown in Fig. 1. This result is confirmed by quantitative analysis that shows that the standard deviation of brightness temperature relative to the symmetric mean is much smaller than that of the typical hurricane for radii within

TABLE 1. A list of annular hurricanes, the basin in which they occurred, the dates (calendar and yearday) during which they exhibited annular hurricane characteristics, and the number of hours they exhibited annular hurricane characteristics. Also listed for reference are the eye size range and the intensity range these storms experienced during each annular phase.

Storm and year	Basin	Annular period (calendar)	Annular period (yearday)	Hours	Eye size range (km)	Intensity range (kt)
Luis, 1995	Atlantic	1800 UTC 3 Sep–0400 UTC 4 Sep	246.75–247.14	10	62–64	120–125
Edouard, 1996	Atlantic	0000 UTC 25 Aug–0000 UTC 26 Aug	238.00–239.00	24	32–35	120–125
Darby, 1998	East Pacific	1200 UTC 26 Jul–1800 UTC 27 Jul	207.50–208.75	30	41–43	90–100
Howard, 1998	East Pacific	1800 UTC 24 Aug–0300 UTC 27 Aug	236.75–239.13	57	44–54	115–85
Beatriz, 1999	East Pacific	1800 UTC 12 Jul–1800 UTC 13 Jul	193.75–194.75	24	41–44	100–105
Dora, 1999	East Pacific	1800 UTC 10 Aug–0300 UTC 12 Aug	222.75–224.13	33	36–38	115–120
		0300 UTC 15 Aug–0300 UTC 16 Aug	227.13–228.13	24	36–39	80–95

the eyewall region. The final feature that is most specific to annular hurricanes is the general lack of deep convective features, including spiral bands, beyond the annulus of deep convection surrounding the eye. Some spiral-shaped features do appear in Fig. 1. However, most of these show characteristics of thick cirrus bands associated with upper-level outflow jets as indicated by the scallops along their edges and the transverse banding seen at cloud top (see Bader et al. 1995, chapter 3), and are likely not associated with near-surface-based, deep convection. The use of IR brightness temperatures in this study however, results in the possibility that spiral bands not visible in IR imagery do exist under the cirrus canopy. The existence of spiral bands is best examined using radar data, which are not available. Passive microwave data could have been utilized for this study, providing single images during the annular phases, but were not. There is at least one example where there is the existence of a spiral band under the cirrus canopy; however, spiral bands are still generally lacking when compared to other intense tropical cyclones.

The annular nature of these storms usually occurs only during a short period of their life cycle. Figure 2 shows time versus radius plots of the azimuthal mean IR brightness temperatures for the Atlantic and eastern Pacific annular hurricanes, with the two Atlantic cases, Luis and Edouard, at the top. Horizontal lines indicate the beginning (earliest) and end (latest) of each annular phase. Also note that Hurricane Dora had two separate annular periods. There are several interesting features in these figures that relate to the shape and behavior of the azimuthal mean brightness temperatures. In the Atlantic (east Pacific) cases, the cold cloud area (< -10°C, shaded in Fig. 2) expands (contracts) as the storms move westward. This is likely related to the SST gradients, where SSTs increase to the west in the Atlantic and decrease to the west in the east Pacific. It is also interesting that the Atlantic storms seem to experience their annular state earlier in their life cycle and have their maximum intensity later, while the eastern Pacific storms transition to an annular state after reaching maximum intensity. However, this interesting observation is far from a conclusion being based upon just six cases. These observations suggest that the environment (i.e., SSTs, vertical wind shear) is likely playing a role in determining the location and frequency of annular hurricanes.

In most of these storms, a strong, diurnal signal in the outward-flowing cirrus canopies occurs in the 200–400-km radial regions, as is documented in Kossin (2002). These diurnal oscillations, examples of which are indicated in Fig. 2 by the letter Ds, appear to suddenly diminish in radial extent in many of these storms during the period when these storms become annular hurricanes. The interesting radial contraction of these oscillations associated with the annular phase of these storms is particularly evident in Howard, Beatriz, and Dora. These oscillations are observed to expand to greater radii following the times that annular characteristics were observed in Luis, Edouard, and Dora and contract with the first eye formation in Darby, Howard, and Beatriz. The transitions both to and from this annular state are rather abrupt. Most evident are the relatively large eye features and the notable decrease in cold cloud features, indicated by brightness temperatures (B_t) between $-10°$ and -60°C, beyond the annulus of deep convection ($B_t \leq -60$°C) surrounding the eye in the region where spiral banding is most often observed in the IR.

b. Intensity characteristics

Typically, hurricanes in the Atlantic experience their peak intensity for very short periods, and then with time fill rather rapidly (Emanuel 2000). In contrast, annular hurricanes subsequent to maximum intensity fill more slowly. In Fig. 3, the time series of intensity, normalized by peak intensity, for typical hurricanes unaffected by

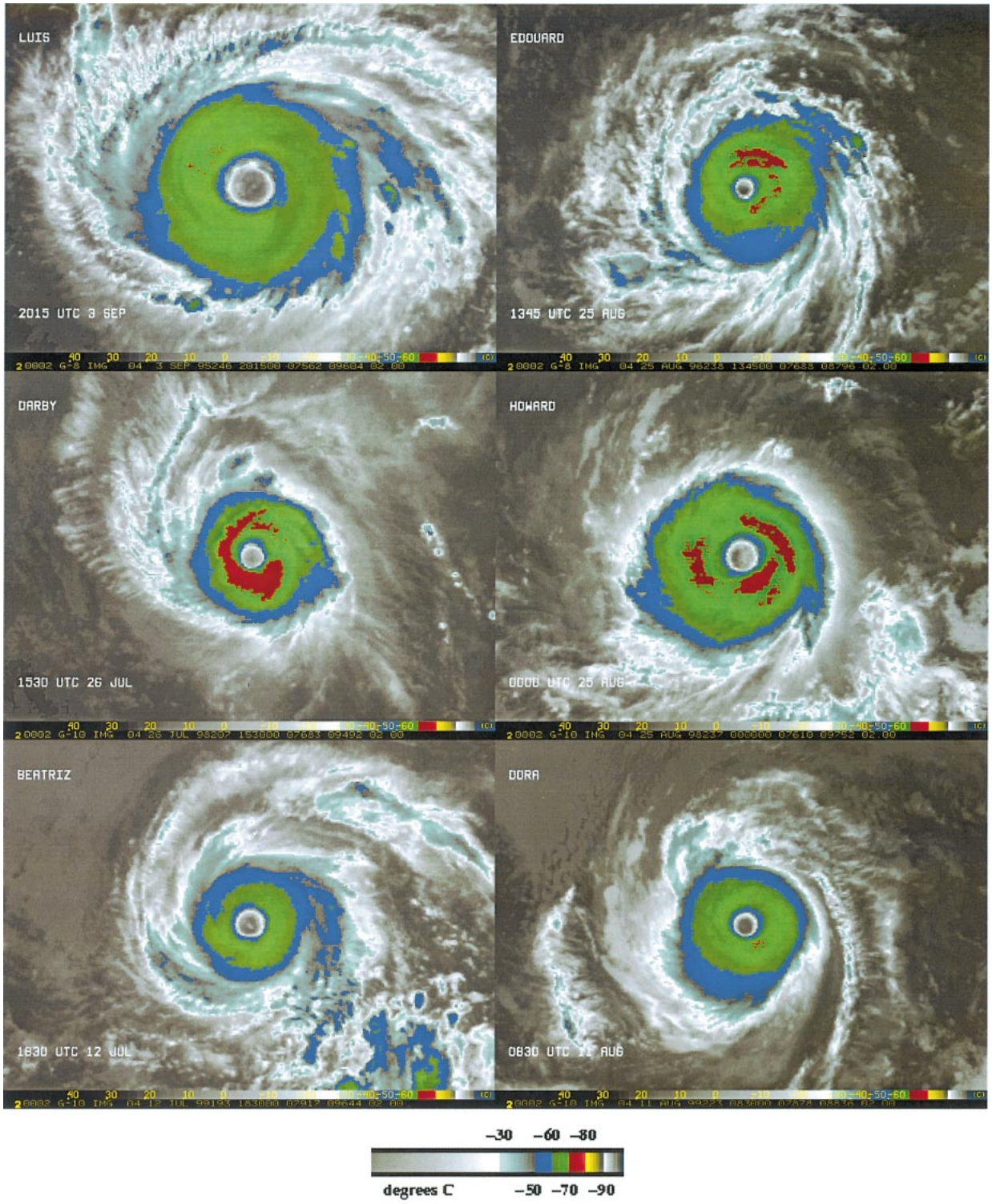

FIG. 1. Color-enhanced IR images of (top left) Hurricane Luis at 2015 UTC 3 Sep, (top right) Hurricane Edouard at 1345 UTC 25 Aug, (middle left) Hurricane Darby at 1530 UTC 25 Jul, (middle right) Hurricane Howard at 0000 UTC 25 Aug, (bottom left) Hurricane Beatriz at 1830 UTC 12 Jul, and (bottom right) Hurricane Dora at 0830 UTC 11 Aug during the period in which they were annular hurricanes. Each image projection is Mercator and has been magnified by a factor of 2 to a 2-km resolution. The resulting spatial scale is 1280 km × 960 km for each panel. The temperature scale for the color enhancement used on the imagery is shown at the bottom.

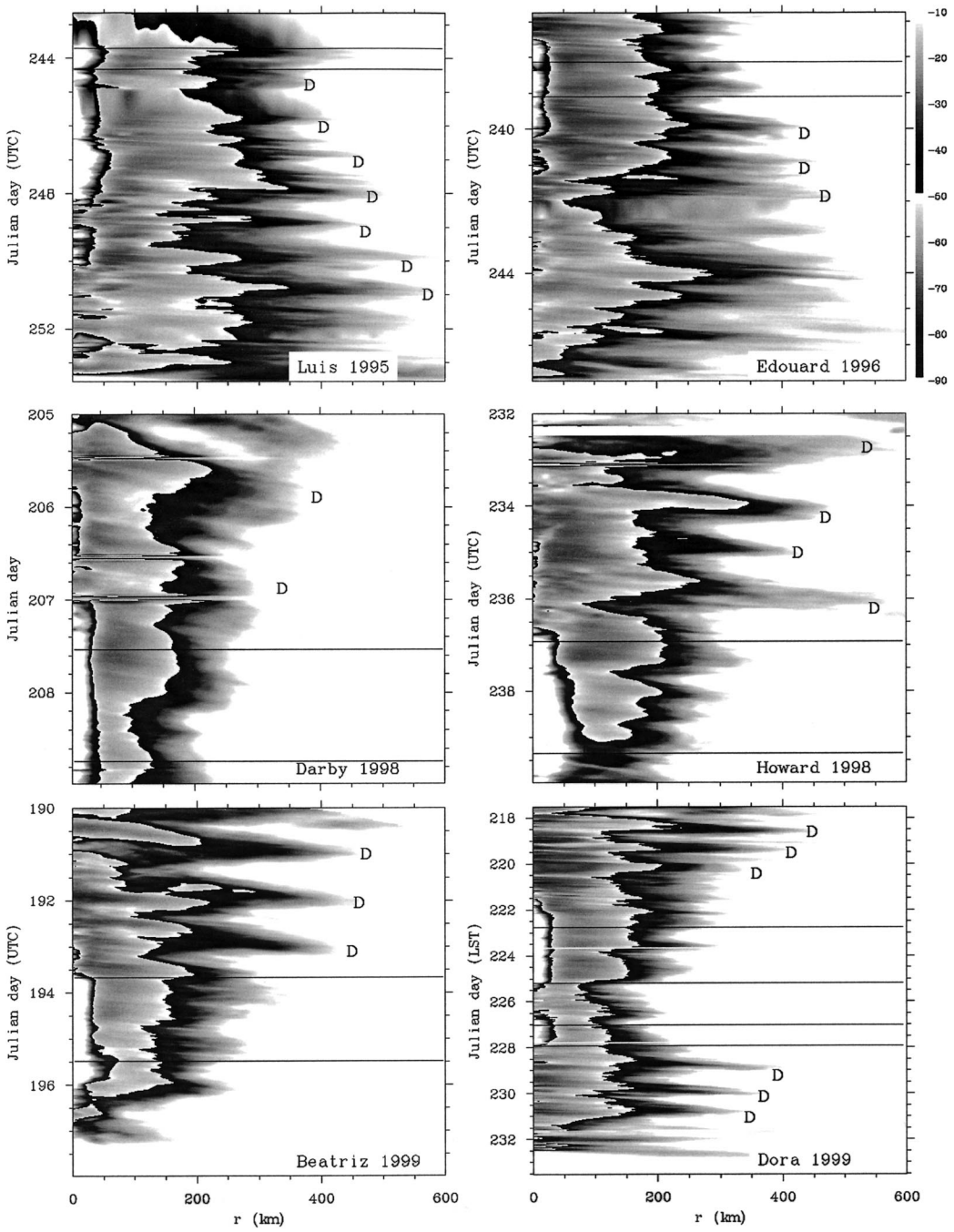

FIG. 2. Time vs radius of azimuthally averaged IR brightness temperature for the entire life cycles of the annular hurricanes listed in Table 1. The top panels display results from the Atlantic annular hurricanes (left) Luis and (right) Edouard. The middle panels display (left) Darby and (right) Howard. The bottom panel shows (left) Beatriz and (right) Dora. The diurnal oscillations discussed in the text, which are located in the 200–400-km radial band, are indicated by a series of Ds at the daily maxima. Horizontal lines indicate the beginning and end of annular periods (see Table 1). Notice that Hurricane Dora had two annular periods and that the timescale is different for each storm.

land or cold water in the Atlantic from Emanuel (2000) is compared with the average time series of intensity of the eastern Pacific and Atlantic annular hurricanes listed in Table 1. Unlike the typical Atlantic hurricane (Emanuel 2000), Fig. 3 shows that annular hurricanes tend to experience a long period of intensity steadiness with a relatively slowly decreasing intensity following their maximum intensity.

The Dvorak (1984) method provides estimates of maximum, average, and slow 24-h weakening rates for

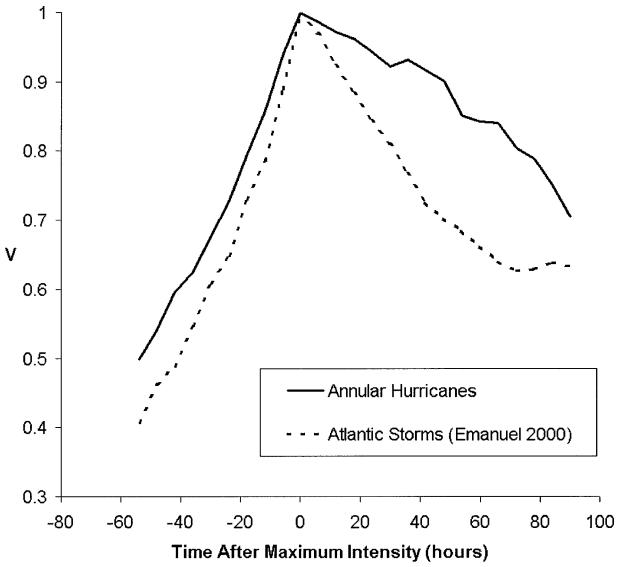

FIG. 3. Composite time series of the intensity (normalized by peak intensity) associated with average Atlantic hurricanes that did not encounter cold water or make landfall (56 cases) as reported by Emanuel (2000) and annular hurricanes (6 cases), normalized by mean maximum intensity. Compositing was done relative to the time of maximum intensity.

storms with similar intensities as the annular hurricanes in this study. The maximum rate of weakening is 1.5 *T* numbers per day, which corresponds to an approximately 40-kt decrease of intensity per day for storms with similar intensities as annular hurricanes. The average (slow) weakening that this method uses is 1 (0.5) *T* numbers per day, which corresponds to approximately 20 kt (12 kt) per day for these same intensities. For instance, for a storm with a maximum intensity of 90 kt, these weakening rates would correspond to 0.61 for maximum weakening, 0.72 for average weakening, and 0.85 for slow weakening at 24 h after maximum intensity in Fig. 3. Note the mean maximum intensity of the sample in Emanuel (2000) is 88.6 kt and the 24-h weakening is 14.7 kt, corresponding to a value of 0.86 in Fig. 3—or slowly weakening. Using the theory discussed in Montgomery et al. (2001) to estimate maximum weakening rates was interesting, producing results remarkably similar to those of Dvorak (1984) (the storm was assumed to have a depth of 15.5 km, the boundary layer was 0.5 km deep, the reduction factor was 0.8, and the drag coefficient was set equal to 2.0×10^{-3}). Using this method a 90-kt storm would weaken nearly 23 kt in 24 h, which in Fig. 3 would correspond to a value of 0.74 at 24 h after maximum intensity. Clearly, annular hurricanes fall in the category of weakening very slowly.

Because the intensity evolution of annular hurricanes is different than that found by Emanuel (2000), the forecast error characteristics are also different. Table 2 shows the average forecast intensity biases and errors for all the cases during the years 1995–99 in the Atlantic and eastern Pacific, along with corresponding biases and errors associated with the annular hurricanes. Results are shown from the SHIPS model and the official NHC forecast at 12, 24, 36, 48, and 72 h. The verification for the Atlantic and eastern Pacific annular hurricanes was performed by restricting the best track to cases 24 h before and 48 h after the annular periods identified in Table 1. The large negative forecast biases associated with these annular hurricanes are shown in both the SHIPS and NHC official forecast verification. The biases range from 10 to 3 times greater than those for the 1995–99 sample. The associated forecast errors are also 10%–40% greater, depending on forecast period. It is also notable that the forecasters (NHC) make remarkably better intensity forecasts than the SHIPS guidance in these cases, apparently by forecasting greater future intensities for these storms. The comparably better NHC forecasts also suggest that an objective technique for identifying annular hurricanes, and conditions associated with their formation, may improve statistically based intensity models such as SHIPS.

c. Annular hurricane formation

Figure 4 shows a sequence of IR images from Hurricane Howard (1998) that depicts one example of an-

TABLE 2. Forecast biases and errors associated with the 1995–99 hurricane seasons in the Atlantic and eastern Pacific as compared with those of the annular hurricanes. Values are represented in knots.

Forecast length (h)	12	24	36	48	72
Forecast biases					
Annular cases (SHIPS)	−4.0	−9.2	−14.8	−20.8	−24.1
Annular cases (NHC)	−2.5	−6.0	−10.8	−17.1	−18.9
No. of forecasts (annular)	110	98	86	74	50
1995–99 (SHIPS)	0.1	0.1	−0.8	−2.1	−3.7
1995–99 (NHC official)	−0.3	−0.8	−1.7	−2.7	−2.3
No. of forecasts (1995–99)	1544	1399	1247	1100	867
Forecast errors					
Annual cases (SHIPS)	9.3	15.0	19.6	23.2	26.7
Annular cases (NHC)	7.5	13.0	17.0	21.8	22.1
1995–99 (SHIPS)	8.1	12.5	15.6	18.2	20.7
1995–99 (NHC)	6.7	11.1	13.8	16.4	19.1

nular hurricane formation. An eye became evident in the IR imagery during 22 August and persisted for more than a day. During this period, the eye was ~12–16 km in diameter (Fig. 4a). At 0630 UTC 24 August, a mass of relatively cloud-free air was observed to intrude into the storm center (Fig. 4b) and subsequently consolidate to form a new, and larger, eye (Fig. 4c). After this time, and during the remainder of 24 August, a rapid and dramatic rearrangement of the IR pattern in Howard's inner core was observed to occur (Figs. 4d–k). At 1530 UTC, the eye–eyewall interface became highly asymmetric as the cold clouds associated with the eyewall appeared to mix inward, and at 1630 UTC, there appeared to be two possible mesovortices rotating together cyclonically around the eye. The nature of mesovortices embedded in a vortex is to act as ''mixmasters''; that is, they efficiently mix the air in their near surroundings. In a nondivergent barotropic framework discussed in Schubert et al. (1999) recently formed mesovortices surrounding the eye mix low potential vorticity located in the eye into the high potential vorticity region associated with the eyewall. One could speculate that this appeared to be occurring during 1700–1900 UTC, as the mesovortices were apparently advecting eyewall air into the eye while orbiting each other in the eye. At the end of this dramatic event (Fig. 4k), the IR pattern was indicative of an annular hurricane, as discussed in section 1a. It is remarkable that in less than 24 h, the diameter of Howard's eye *increased by a factor of more than 4* as the eye diameter increased from ~12 to ~88 km.

Another example of annular hurricane formation is offered in Fig. 5, which shows the transition of Hurricane Luis (1995) into an annular hurricane. The transition of Luis is less dramatic, but has several similarities to Howard. In Fig. 5a Luis has a nearly circular eye and one major spiral band to its north and northeast. There also appears to be an undulation along the inner eyewall of the storm in Fig. 5a, possibly indicating the existence of a mesovortex. An hour latter (Fig. 5b), there is an elongated region of warmer cloud-top temperatures to the north and northeast of the eyewall that appears associated with aforementioned mesovortex feature that has now rotated to the northeast inner eyewall. In Fig. 5c the warm cloud tops are associated with a noticeable break in the eyewall, which over the next 4 h (0915–1315 UTC; Figs. 5d–i) rotates around the storm center, displaying at times what could be described as a banded eye structure. An hour latter (1415 UTC; Fig. 5j), a large area of cold cloud appears in the inner southeast region of the eyewall, which dissipates as it rotates around the eye, as shown in Fig. 5k, 3 h later. Over the next 3 h the eye expands to have a diameter of ~120 km, increasing by a factor of approximately 2.

Although the specific details can vary between the annular cases, rearrangements involving possible mesovortices were observed in all of the other annular hurricanes considered in this study with storms undergoing a similar succession of events with one or two possible mesovortices transforming a smaller eye into a larger eye. Luis, Edouard, and Dora had one possible mesovortex associated with their transition while Howard, Darby, and Beatriz had two of these features that were associated with their transition to an annular hurricane. The transition timescales of these cases were quite similar with most transitions taking ~24 h. The storms that had two possible mesovortices appeared to undergo transition in a more dramatic fashion in the IR imagery while transitions involving one mesovortex appeared to be less abrupt.

All of these transitions could be viewed as an eyewall replacement process (i.e., a smaller eyewall is replaced by a larger eyewall). While the formation of concentric eyewalls is likely a symmetric process (e.g., Willoughby et al. 1982), and the mechanisms that cause the formation of concentric rings of convection and tangential winds are still in dispute, the dissipation of the primary eyewall once the outer eyewall has become dominant has been has been modeled using simple 2D barotropic dynamics (Kossin et al. 2000). The results of this modeling effort show that the existence of a secondary ring of elevated vorticity (secondary eyewall) along with its strength and proximity to the inner vorticity maximum (primary eyewall) affects the details of the dissipation of the primary eyewall. Several long-lived structural configurations can result, including long-lived vorticity rings (i.e., eyewalls) near the radii of the initial secondary vorticity maximum.

Radial profiles of vorticity and θ_e from Hurricanes Luis and Dora, the only storms with reconnaissance data available during their annular phase, are rather intriguing. Figure 6 shows the tangential wind, angular velocity, θ_e, and vorticity for Hurricane Luis for the radial legs occurring between 2230 and 2308 UTC 3 September. These profiles are very similar to those of Hurricane Dora (not shown for brevity), nothing that Dora was a smaller and weaker annular hurricane when observed by reconnaissance aircraft on 15 August. The tangential wind (v) has a U-shaped profile (i.e., $\partial^2 v/\partial r^2 > 0$) with a number of visible steplike features as the profile transitions from the middle of the eye to the radius of maximum wind with a very steep transition occurring just inside the radius of maximum wind. In the angular velocity and vorticity fields, the steplike features in the tangential winds appear as local maxima and thus the Rayleigh necessary condition for barotropic instability is satisfied. The θ_e indicates that the eyewall is generally well mixed with respect to this conserved variable, with local maxima and minima roughly corresponding to the local minima and maxima in the angular velocity field. These steplike features in the tangential winds may be evidence of PV filamentation (e.g., Ritchie and Holland 1993). In the context of a recent paper by Kossin and Eastin (2001), the annular hurricanes seem to be neither in regime 1 (barotropically unstable) nor in regime 2 (barotropically stable), but rather in between these regimes. Evidence that a dramatic PV mixing event has

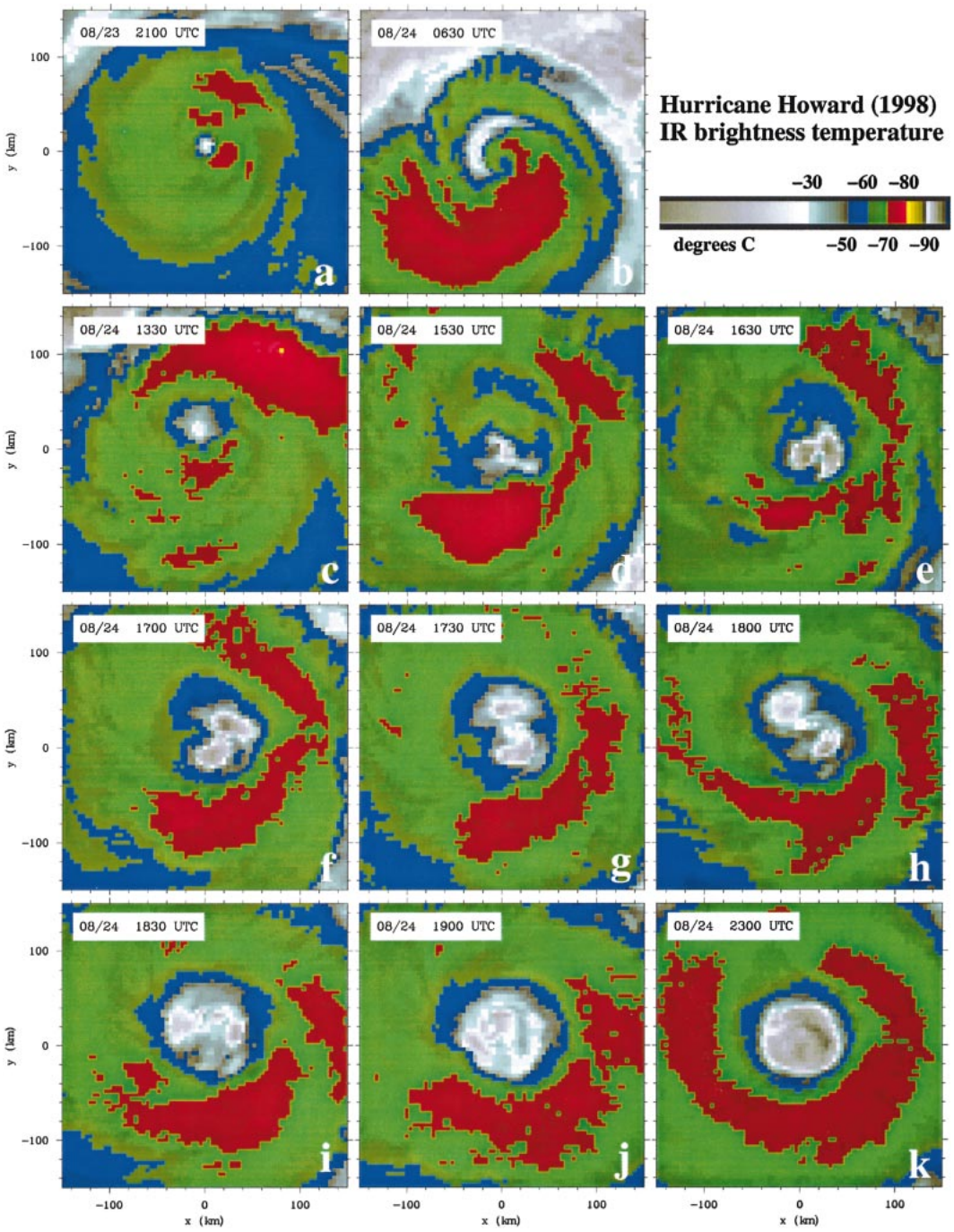

FIG. 4. The transition of Hurricane Howard from a hurricane with a small eye (~12 km diameter) to an annular hurricane. Times on the individual panels are shown in the upper left of each panel and the temperature enhancement used in all the images is shown in the upper-right panel of this figure. Description of the evolution is given in the text.

→

FIG. 5. The transition of Hurricane Luis to an annular hurricane. Times are shown in the bottom center of each panel and the temperature enhancement used in all the images is shown at the bottom of this figure. Description of the evolution is given in the text.

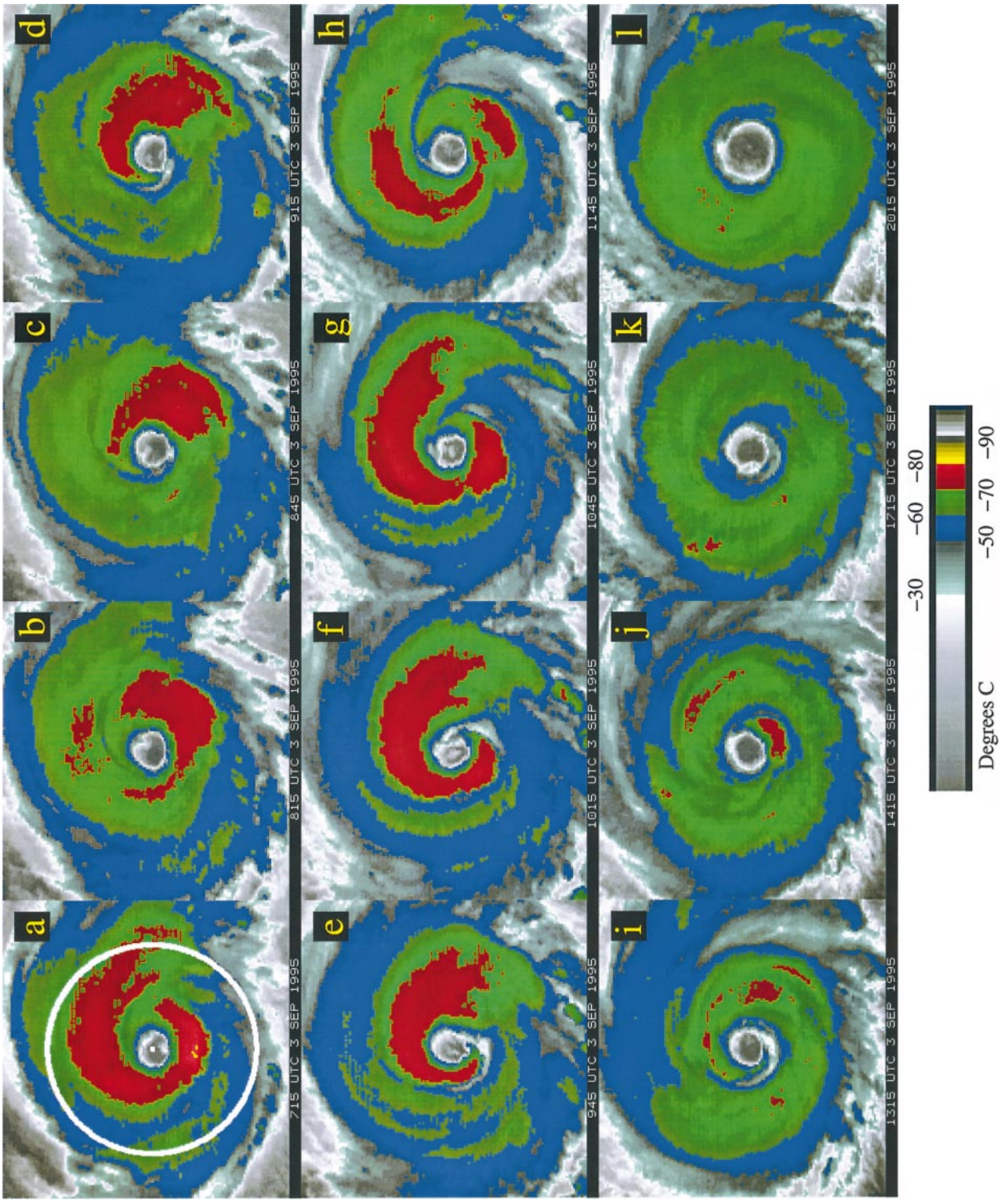
a
b
c
d
e
f
g
h
i
j
k
l
715 UTC 3 SEP 1995
815 UTC 3 SEP 1995
845 UTC 3 SEP 1995
915 UTC 3 SEP 1995
945 UTC 3 SEP 1995
1015 UTC 3 SEP 1995
1045 UTC 3 SEP 1995
1145 UTC 3 SEP 1995
1315 UTC 3 SEP 1995
1415 UTC 3 SEP 1995
1715 UTC 3 SEP 1995
2015 UTC 3 SEP 1995
-30 -60 -80
-50 -70 -90
Degrees C

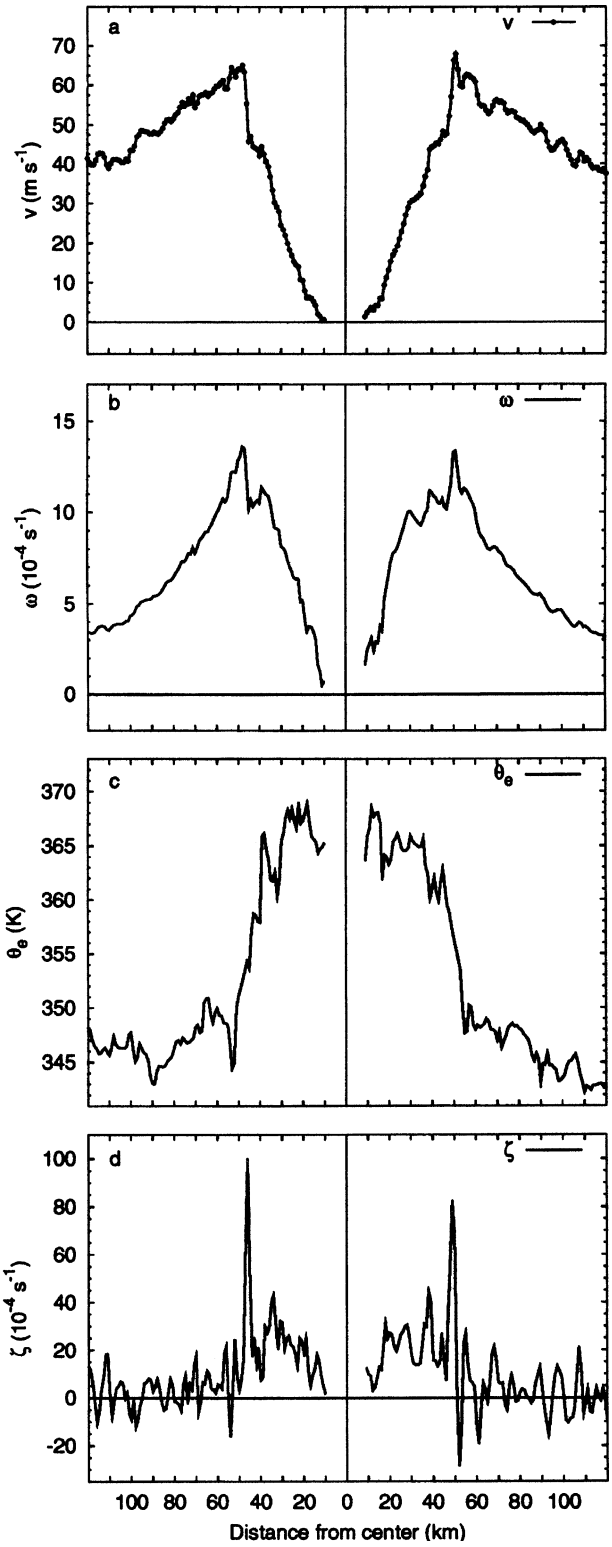

FIG. 6. Cross sections of (a) tangential wind, (b) angular velocity, (c) θ_e, and (d) vorticity calculated from flight-level (10 000 ft) reconnaissance data of Hurricane Luis for 2230–2308 UTC 3 Sep 1995.

occurred is shown by the nearly uniform eye θ_e values. However, a U-shaped tangential wind field is evidence that the possibility for barotropic instability still exists. The existence of this wind profile coupled with the observation of the relatively long-lived nature of annular hurricanes allows us to speculate that as the vorticity is continuously being increased in association with the convection near the eyewall, it also may be being mixed contemporaneously into the eye by possible PV filamentation as indicated in the radial profiles.

This limited evidence produces more questions than it answers. Though some of the dynamic and thermodynamic structure of annular hurricanes can be observed using reconnaissance data, the three-dimensional details of the formation of annular hurricanes are well beyond both the scope of this paper and the quality of the presently available data. The existing evidence suggests that annular hurricane formation is likely preceded by a dramatic horizontal mixing event as shown in Figs. 4 and 5. The mixing probably results in fairly uniform radial profiles of θ_e in the larger than average eye of an annular hurricane. It also appears as if the mixing process is on going as indicated by the local maxima and minima in the angular velocity and vorticity fields. Interestingly, the evidence of continued mixing may help to explain the nearly steady intensities associated with annular hurricanes, but the existing observations do not contain enough quantitative detail to further investigate these processes. We also know that all storms that develop barotropic instability do not become annular hurricanes, which implies that in addition to barotropic instability, other conditions must be satisfied. With this in mind, the next section discusses environmental conditions associated with annular hurricanes.

d. Typical environmental conditions

The environmental conditions associated with the annular phase of each of the hurricanes listed in Table 1 are examined using 12-hourly data derived from NCEP operational atmospheric and oceanic analyses as described in section 2. Specifically, they include SST, 200-hPa zonal winds, 200-hPa temperatures, vertical wind shear in a deep layer (200–850 hPa) and a shallow layer (500–850 hPa), 850-hPa vorticity, 200-hPa divergences and 200-hPa REFC. Also calculated for this study are the maximum potential intensity (MPI)[2] of the hurricane based upon SST [method of DeMaria and Kaplan (1994b)], storm intensity, and intensity as a percentage of MPI. All environmental values, except SST and vertical wind shear, are area averaged within a 1000-km circle. Wind shear calculations are averaged within a 600-km circular area and SST values are calculated at

[2] Note that the values for MPI in the 25.4°–28.5°C temperature range are not much different (1–6 kt greater) from values obtained using the method of Whitney and Hobgood (1997), developed specifically for the eastern Pacific.

the storm center. For interpretation purposes, positive 200-hPa REFC indicates that the storm-relative asymmetric radial and tangential winds, resulting from the storm interacting with the environment, are negatively correlated resulting in a positive tangential wind tendency at 200 hPa (e.g., REFC is positive and large when the storm moves toward an upper-level trough).

Table 3 compares the environmental conditions of the annular hurricanes with those of the combined 1995–99 Atlantic and eastern North Pacific sample. This table helps to determine the ranges of observed values as well as the assignment of statistical importance of the means. Statistical significance of the means in determined using the Student's *t* test and a 95% confidence level. Statistical significance in Table 3 is indicated by the use of boldface italic print. The mean intensity of these annular hurricanes (107.6 kt) is significantly stronger than the sample mean. Average SSTs for annular hurricanes were 26.9°C with a much smaller range of values than the sample mean, yet the mean is not significantly different than the sample. Despite the rather modest values of SSTs, all of the annular hurricanes had cloud-top temperatures colder than −55°C at all times, indicating that the tops of clouds are at their lowest near 200 hPa. Also, in all of the cases the SSTs are fairly constant with a tendency to decrease with time. Annular hurricanes have intensities that are 83.5% of their MPI, much larger than the sample mean of 42.5%, suggesting that the environment is very conductive to tropical cyclone maintenance. This contention is supported by the average vertical wind shear, which is small in both the deep layer (850–200 hPa) and the shallow layer (850–500 hPa). The zonal and meridional components of the vertical wind shears in these two layers indicate that the shear associated with annular hurricanes is easterly for the deep layer and east-southeasterly for the shallow layer. The 200-hPa mean zonal winds associated with annular hurricanes are also statistically significant and easterly, with a mean value of −5.0 m s^{-1} and standard deviation of 1.2 m s^{-1}. Likewise, the 200-hPa mean temperatures are colder than the sample mean. The values of 200-hPa REFC are very near zero, which is also true for the sample mean, and showed little variability, indicating interactions with the environment, particularly upper-level troughs, are likely not important. The conditions at 200 hPa suggest a location in the Tropics, slightly equatorward of an upper-level ridge.

There are eight environmental factors that are associated with all the annular hurricanes in this study. These factors are listed in Table 4 with their acceptable ranges, which are derived from the observed means plus or minus two standard deviations (~95% confidence with $n = 25$). Also listed in Table 4 are the percentages that each of these conditions existed in each basin as determined during the years 1989–99 in the NCEP analyses. The final row of Table 4 lists the percentage of time all eight environmental conditions existed simultaneously in each basin in the same analyses. Individually the

Table 3. Average environmental conditions associated with the individual cases of Atlantic and eastern Pacific annular hurricanes along with the 1995–99 sample mean values. Listed are temperatures, wind speeds, two layers of total zonal and meridional vertical wind shears, maximum potential intensity (MPI), intensity, storm REFC, 850-hPa vorticity, and 200-hPa divergence. Units of these quantities are listed in the column headings. "Deep" and "shallow" in the table refer to values of wind shears between levels 200 and 850 and 500 and 850 hPa, respectively. Boldface italic indicates statistical significance.

	SST (°C)	200-hPa U (m s^{-1})	200-hPa T (°C)	Deep shear (m s^{-1})	Deep U (m s^{-1})	Deep V (m s^{-1})	Shallow shear (m s^{-1})	Shallow U (m s^{-1})	Shallow V (m s^{-1})	200-hPa REFC (m s^{-1} day^{-1})	200-hPa divergence (10^{-6} s^{-1})	850-hPa vorticity (10^{-6} s^{-1})	MPI (kt)	Intensity (kt)	%MPI
Annular hurricanes (sample size = 25)															
Mean	26.9	***−5.0***	***−55.7***	***2.7***	***−2.6***	0.7	2.8	***−2.6***	***1.0***	0.0	22	41	***128.9***	***107.6***	***83.5***
Std dev	0.8	***1.2***	***0.5***	***1.9***	***2.3***	2.1	1.2	***1.2***	***1.1***	0.4	25	38	***8.9***	***12.0***	***7.6***
Max	28.5	***−2.9***	***−54.5***	***7.4***	***1.2***	5.9	4.8	***0.1***	***3.1***	1.0	75	101	***148.9***	***125***	***95.9***
Min	25.4	***−6.9***	***−56.5***	***0.8***	***−6.4***	−2.6	0.8	***−4.7***	***−0.7***	−1.0	−20	−30	***113.2***	***90***	***66.0***
1995–99 sample mean (sample size = 1516)															
Mean	27.6	0.9	−55.3	7.1	2.4	−0.1	3.2	0.2	0.2	1.1	24.6	29	139.3	58.3	42.5
Std dev	1.8	6.6	1.0	4.1	6.7	4.1	1.8	3.2	1.7	3.3	23.4	45	19.26	28.3	20.7
Max	30.8	26.9	−52.7	24.4	24.4	16.5	0.1	11.3	7.6	20.0	126	190	165.0	155.0	97.4
Min	19.1	−14.9	−60.3	0.1	−17.0	−13.8	12.1	−9.6	−5.5	−16.0	−39	−111	81.51	20.0	12.6

TABLE 4. List of the eight environmental conditions derived from the 1989–99 NCEP analyses associated with annular hurricanes. Listed is the condition on the left followed by the percentage of occurrence in association with tropical cyclones in each basin. The number of 12-hourly cases that existed in each basin during this 12-yr period is given in parentheses. Ranges for the environmental conditions are determined from Table 3 (the means plus or minus two standard deviations). The last category (all) refers to the percentage of time all eight of the factors existed at the same time, as is the case with the six annular hurricanes examined in this study. The all category represents the percentage of time that environmental conditions conducive to the formation of annular hurricanes have existed in each basin.

Parameter	Atlantic (1424) (%)	East Pacific (1876) (%)
1) Weak vertical wind shear, deep shear < 6.5 m s^{-1} and shallow shear < 5.2 m s^{-1}	41.5	67.5
2) Easterly 200-hPa U, $2.5 > U > -7.4$ m s^{-1}	13.1	42.9
3) 200-hPa T, $-54.7 > T > -56.7$°C	70.8	64.9
4) Environmental interaction, |REFC| < 2 m s^{-1} day^{-1}	46.9	76.8
5) SSTs, $25.2 >$ SST > 28.6°C	63.6	50.8
6) Easterly deep shear $2 > U > 7.2$ m s^{-1}	25.0	67.5
7) Southeast shallow shear, $-0.2 > U > -5.0$ m s^{-1}, $3.2 > V > -1.2$ m s^{-1}	13.5	51.7
8) Intensity VMAX > 85 kt	16.5	21.1
All (1–8)	0.8	3.0

conditions associated with annular hurricanes are quite common, with the most limiting overall factor being intensity. However, the simultaneous combination of the environmental conditions shown to be associated with annular hurricanes is quite rare in both basins during the 1989–99 period, with 0.8% and 3.0% of the cases exhibiting these conditions in the Atlantic and eastern Pacific basins, respectively. It is interesting to note that the percentages of easterly 200-hPa zonal wind as well as easterly shear are about three times higher in the eastern Pacific than in the Atlantic. This climatological difference coupled with a greater number of storms occurring annually in the east Pacific likely would explain the greater possibility of annular hurricane occurrence in that basin.

Using the 36-h period following the annular phases of these six hurricanes, seven periods in all (since Dora experienced two annular periods) were examined to determine what environmental factors changed that possibly caused the demise of each annular phase. Using the eight factors and the ranges for each listed in Table 4, Table 5 was constructed. For the 36-h period following each annular hurricane's demise the NCEP analyses are examined to determine if the eight environmental factors are within the ranges expected for annular hurricanes. If an environmental factor is out of range, an X is placed in the table for that factor. Dora I and Dora II refer to the first and second annular periods for Hurricane Dora. In most case the directional component of either or both of the 200–850-or the 500–850-hPa shear was related to the demise of these annular hurricanes including Luis, Edouard, Beatriz, Howard, and Dora (I and II). In the case of Luis, Edouard, and Dora II, westerly 200-hPa winds accompanied these changes. In the case of Dora I, 200-hPa winds became too easterly. Howard became asymmetric as it encountered modest northeast wind shear in the 500–850-hPa layer as it also encountered colder water. Beatriz, during its encounter with colder water, slowed and was sheared too strongly from the east in the 500–850-hPa layer. Dora I lost its annular characteristics when it experienced a period of southerly shear, while the demise of Darby appears to be solely related to that storm encountering cold water. As anticipated the vertical wind shear direction and magnitude appears to play a roll in the demise of annular hurricanes while the SST seems to also be a factor, too warm in Luis and too cold in Howard, Beatriz, and Darby.

According to these observations, the typical annular hurricane has an intensity of approximately 85% of its empirically derived MPI and exists in a favorable hurricane environment characterized by 1) weak easterly or southeasterly vertical wind shear, 2) easterly flow and relatively cold temperatures at 200 hPa, 3) occurrence within a narrow range (25.4°–28.5°C) of SSTs that are nearly constant, and 4) a lack of 200-hPa relative eddy flux convergence caused by the environment. Furthermore, as the environment changes and the environmental factors listed in Table 4 are no longer satisfied, particularly the vertical wind shear (direction and magnitude), and to a lesser degree the SST, these storms loss their annular characteristics.

4. Objective identification techniques

The annular hurricane cases listed in Table 1 were determined by the visual inspection and qualitative evaluation of the IR imagery. Because annular hurricanes have intensities greater than 85 kt and display intensity change characteristics that are different from the average hurricane resulting in significant intensity forecast errors, their identification in an operational setting would likely be useful for improving intensity forecasts. While the subjective identification method used in this study is adequate for the purposes of describing annular hurricanes and their environments in a postanalysis setting, there is a need for a systematic and objective technique for identifying these storms. Building on the characteristics of annular hurricanes discussed in section 3, the development of two objective identification techniques is explored in this section.

The first approach is to use the digital values of the IR imagery to create an index. Figure 2 shows that the radial extent of the cirrus canopy, indicated by the cold values of azimuthally averaged IR temperatures, is much smaller and that there is evidence of a warm eye feature

TABLE 5. Table illustrating what factors were related to the demise of each annular phase of the six annular hurricanes listed in Table 1. Listed across the top are the eight environmental conditions, labeled 1–8, which correspond to the same labels in Table 4, that are found to be consistently present during the annular phases of these storms. Listed are the three 12-hourly analyses following each annular period. An X in a column indicates that the condition associated with that column is no longer being satisfied; see Table 4 for explanation of the conditions associated with each column.

Hours	1 Shear magnitude	2 *U*200	3 200-hPa temp	4 REFC	5 SST	6 Easterly 200–850-hPa shear	7 Southeast 500–850-hPa shear	8 Intensity
				Luis				
+12						X	X	
+24						X	X	
+36	X	X		X	X	X	X	
				Edouard				
+12						X		
+24						X		
+36	X					X	X	
				Darby				
+12					X			
+24					X			
+36					X			X
				Howard				
+12			X				X	
+24			X		X		X	X
+36			X		X		X	X
				Beatriz				
+12							X	
+24					X		X	
+36					X	X	X	
				Dora I				
+12							X	
+24		X					X	
+36		X					X	
				Dora II				
+12						X	X	
+24		X				X	X	
+36		X				X	X	

during the annular hurricane periods (see Table 1 for exact times). Using the information shown visually in Fig. 2, a simple index can be created by comparing the azimuthally averaged radial profiles of IR brightness temperature with the average profiles of the annular hurricanes. Since annular hurricanes have different sizes and have different ranges of IR temperatures associated with their cloud tops as shown in Fig. 2, the profiles of azimuthally averaged IR temperature need to be normalized to a common size and a common average cloud-top temperature. The brightness temperatures are normalized by subtracting the $r = 0$ to $r = 444$ km radial average of the azimuthally averaged brightness temperature ($\overline{\langle B_t \rangle}$) from the azimuthally averaged brightness temperature at each radii ($\langle B_t(r) \rangle$), creating an anomaly value (b_t):

$$b_t = \langle B_t(r) \rangle - \overline{\langle B_t \rangle}. \quad (2)$$

The normalized radius (R) is created by subtracting the radius of the coldest azimuthally averaged brightness temperature within 600 km of the radius ($r_{Bt\ \min}$) from the physical radius (r) and dividing by the $r_{Bt\ \min}$:

$$R = \left(\frac{r - r_{Bt\ \min}}{r_{Bt\ \min}} \right). \quad (3)$$

These procedures result in a normalized radial profile of normalized brightness temperature where the coldest normalized brightness temperature is located at the origin of normalized radius ($R = 0$). The averaged normalized radial profile of normalized brightness temperature (i.e., R versus b_t) along with the normalized radial profiles of normalized brightness temperature of the six annular hurricanes that make up the average are shown in Fig. 7.

In order to compare a given azimuthally averaged brightness temperature profile to the average one shown in Fig. 7, referred to as the mean profile, an identical normalization procedure must be performed on the azimuthally averaged IR brightness temperature profile of

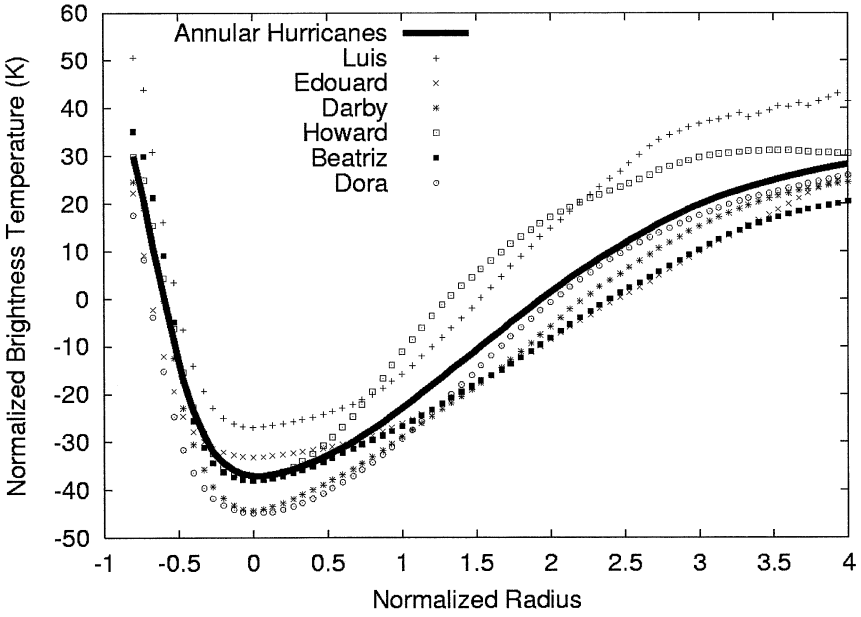

FIG. 7. Average normalized radial profiles of normalized brightness temperatures for each annular hurricane along with the six-storm average indicated by the thick dark line. See text for the radius and temperature normalization procedures.

the tropical cyclone image under consideration or the test profile. The comparison is accomplished by 1) computing the amount of the variance the test profile explains in the mean profile, 2) calculating the mean absolute temperature difference between the mean and test profiles, and 3) testing for a large warm eye in the imagery. Using dependent data from the six annular hurricanes involved in this study, it was found that a value of 50% of explained variance and a mean absolute difference of 14°C did a proficient job of distinguishing the annular phase of these hurricanes from the rest of their life cycle. Using the imagery of the storms listed in Table 1, it was also found that a large warm eye could be distinguished using the radial profile of azimuthally averaged brightness temperature. The existence of a large warm eye requires that the radius of the coldest azimuthally averaged brightness temperature ($r_{Bt\,\min}$) be greater than 54 km and that the warmest brightness temperature inside $r_{Bt\,\min}$ be warmer than 0°C. In evaluating the imagery, the annular hurricane index was set to a value of 1.0 if all of these requirements were met for a 3-h period of time and otherwise assigned a value of 0.0.

Figure 8 shows time series plots of this simple index along with the times listed in Table 1 (dark horizontal bar) for the six hurricanes discussed in this study. This method proved dependable in identifying the annular hurricane phases of the six storms that made up the dependent sample included in this study, particularly those occurring in the eastern Pacific basin, noting that the IR datasets for Luis and Edouard were of a slightly poorer quality. Although the times where the index was positive did not exactly line up with the subjective times, the index did identify each storm. This objective method was also evaluated on all of the storms in the IR tropical cyclone archive through 1999. The storms that were identified by this method as being annular are listed in Table 6 along with the number of hours they were identified as having annular characteristics. In these diagnostic trials, 17 storms were identified as having annular characteristics out of a possible 63 hurricanes and only 6 were subjectively identified as being annular hurricanes (i.e., Table 1). This evaluation indicates that this method correctly classifies hurricanes as being annular or not 52 out of 63 times (83% of the time). The exact time of annular occurrence however proved more difficult to predict with a success rate of approximately 25%. Reviewing the imagery associated with these 17 storms, most of the false alarms are associated with two factors: 1) large warm eyes with ragged edges that appear in the azimuthal average as symmetric (i.e., Felix, Hortense, Nora, Kay, Cindy, and Gert) and 2) very intense hurricanes (i.e., Guillermo, Mitch, and Floyd). Interesting is the observation that these storms, while clearly not annular hurricanes, experiences rather steady intensities during these times. On the other hand, Georges was considered when the storms in the IR archive were being subjectively evaluated, and had many of the characteristics of an annular hurricane, but it was not selected because its eye was a little smaller than average and was continuously contracting during the period it displayed an annular ring of convection with little spiral band activity.

The second approach to creating an objective method

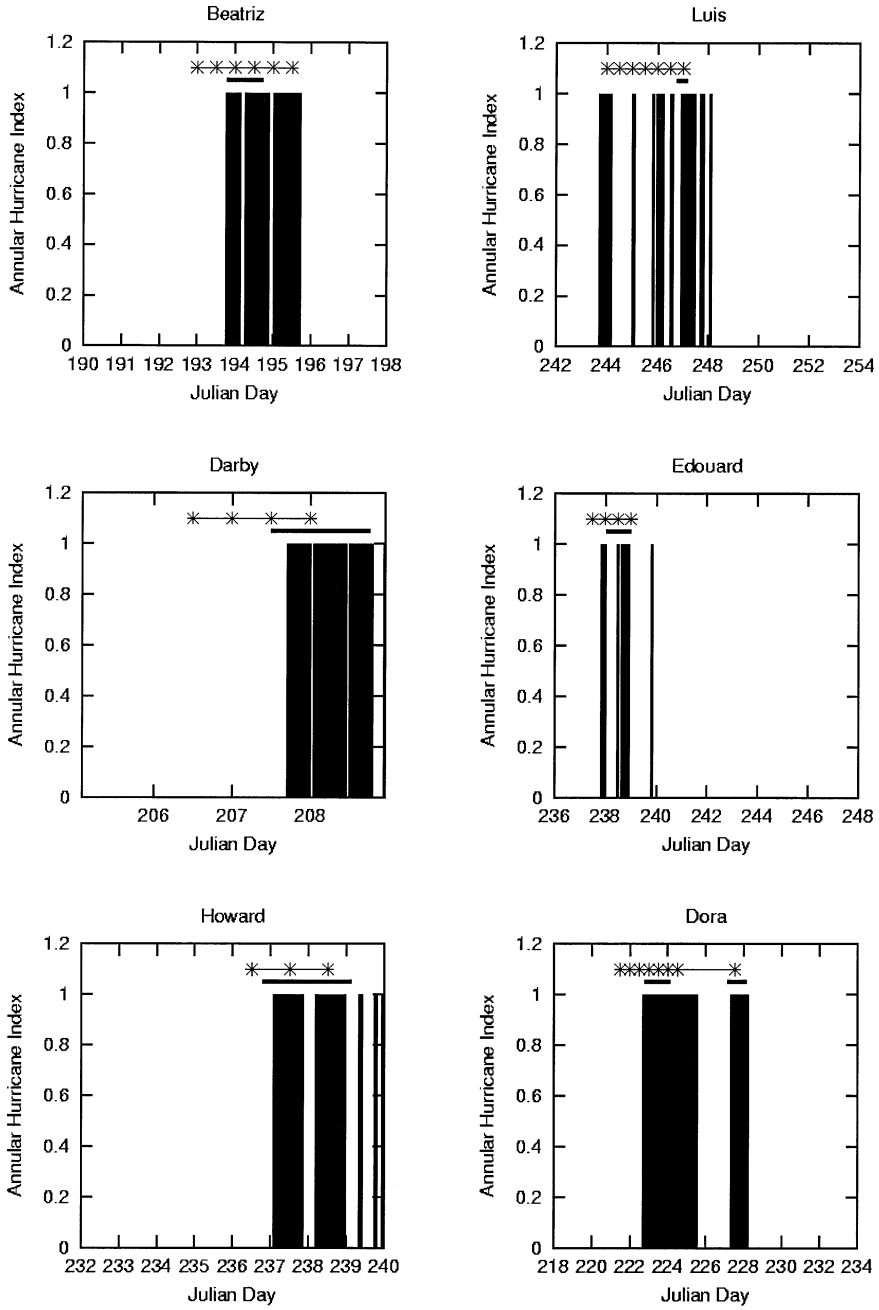

FIG. 8. Results of the objective annular hurricane indices are shown along with the annular hurricane periods determined from a subjective analysis of IR data. A thick horizontal bar indicates the subjectively determined time periods for each annular hurricane (i.e., those in Table 1). The vertical bars indicate the results from the objective IR annular hurricane index, where a value of 1 indicates that an annular hurricane exists according to the rules of this index. Also shown are the 12-hourly results of the environmental annular hurricane index, which are indicated by asterisks at each 12-h point where the environmental conditions were found favorable for annular hurricanes. Thin lines connect the asterisks if these conditions last longer than one 12-h period.

for identifying annular hurricanes is to inspect the environmental conditions for times when the environmental conditions associated with annular hurricanes exist. Table 4 lists the required environmental conditions for annular hurricanes along their expected ranges, as shown in Table 3.

Using the same 1989–99 data, a search for time periods during which all of these environmental factors

TABLE 6. A list of storms identified as annular using the digital IR values in the imagery. Listed is the year, the storm name, the basin, the dates and times of identification, and the number of hours contained in each period.

Year	Storm	Basin	Dates	Hours
1995	Felix	Atlantic	0600 UTC 20 Aug–1000 UTC 20 Aug	5
1995	Luis	Atlantic	1800 UTC 31 Aug–0400 UTC 1 Sep	11
			0300 UTC 3 Sep–0500 UTC 3 Sep	3
			2200 UTC 3 Sep–1100 UTC 4 Sep	14
			1700 UTC 4 Sep–1900 UTC 4 Sep	3
1996	Edouard	Atlantic	2300 UTC 24 Aug–2200 UTC 25 Aug	24
1996	Hortense	Atlantic	2200 UTC 12 Sep–0100 UTC 13 Sep	4
1997	Guillermo	East Pacific	1400 UTC 5 Aug–1500 UTC 5 Aug	2
			1900 UTC 5 Aug–2000 UTC 5 Aug	2
1997	Nora	East Pacific	0200 UTC 22 Sep–1500 UTC 22 Sep	14
1998	Georges	Atlantic	1300 UTC 19 Sep–0900 UTC 20 Sep	21
1998	Mitch	Atlantic	1600 UTC 26 Oct–0100 UTC 27 Oct	10
1998	Darby	East Pacific	1700 UTC 17 Jul–1900 UTC 18 Jul	26
1998	Georgette	East Pacific	1300 UTC 14 Aug–2100 UTC 14 Aug	9
1998	Howard	East Pacific	0200 UTC 25 Aug–1900 UTC 25 Aug	18
			0500 UTC 26 Aug–2300 UTC 26 Aug	19
			0800 UTC 27 Aug–1000 UTC 27 Aug	3
1998	Kay	East Pacific	0500 UTC 15 Oct–1000 UTC 15 Oct	6
1999	Cindy	Atlantic	2300 UTC 27 Aug–1700 UTC 28 Aug	19
1999	Floyd	Atlantic	0000 UTC 13 Sep–0400 UTC 13 Sep	5
			1300 UTC 14 Sep–1700 UTC 14 Sep	5
1999	Gert	Atlantic	1600 UT 18 Sep–0400 UTC 19 Sep	13
1999	Beatriz	East Pacific	1900 UTC 12 Jul–0300 UTC 13 Jul	9
			0700 UTC 13 Jul–2100 UTC 13 Jul	15
			0100 UTC 14 Jul–1700 UTC 14 Jul	17
1999	Dora	East Pacific	1700 UTC 10 Aug–0200 UTC 12 Aug	35
			0800 UTC 12 Aug–1200 UTC 12 Aug	5
			1500 UTC 12 Aug–1200 UTC 13 Aug	22
			0800 UTC 15 Aug–2200 UTC 15 Aug	15
			0900 UTC 16 Aug–1100 UTC 16 Aug	3

TABLE 7. A list of annular hurricanes identified by the simultaneous existence of all of the environmental conditions associated with annular hurricanes, which are listed in Table 4. Listed are the year, the storm's name, and the number of 12-h periods for which these conditions existed in the environment.

Year	Storm	No. of 12-h periods
1989	Ismael	1
	Octave	1
	Raymond	3
1990	Hernan	2
	Iselle	4
	Marie	2
	Odile	1
1992	Frank	3
	Georgette	4
	Orlene	1
1993	Jova	2
	Kenneth	1
	Lidia	2
1995	Barbara	6
	Luis	7
1996	Douglas	1
	Edouard	4
1998	Darby	4
	Howard	3
1999	Beatriz	5
	Dora	9
	Eugene	1

are occurring simultaneously forms the basis of an objective technique for identifying annular hurricanes. Using this environmental index for the years 1989–99, 22 storms were identified as having environmental conditions similar to annular hurricanes, 20 of which occurred in the eastern Pacific, as shown in Table 7. In the Atlantic, the only storms identified where Luis and Edouard. It also appears that there are certain years when the environment is conducive to annular hurricane formation. An interesting sidebar is the observation that annular hurricanes in the eastern Pacific are more likely to occur in years when the eastern and central equatorial Pacific have negative SST anomalies.

Unfortunately, it is impossible to verify this method since the IR archive does not exist prior to 1995 in the Atlantic and 1997 in the east Pacific. It is, however, noteworthy that during the period when IR data were available that of the 63 hurricane cases, only 1 case was misidentified (Eugene 1999), suggesting this method is dependable. Figure 8 illustrates the periods identified using this method as asterisks for each 12-hourly positive index values. If more than one consecutive 12-hour period is identified, the asterisks are connected with a thin line. Results from this index show that the environmental conditions seem to lead the formation of annular hurricanes as determined subjectively (i.e., Ta-

ble 1) and by the objective (IR) method (i.e., Table 4). This observation is consistent with recent theoretical work (e.g., Jones 1995; Bender 1997; Frank and Ritchie 1999, 2001) that show that wind shear is not only the major modulator of asymmetric and axisymmetric convective structure in hurricanes, but also that the structural changes lag the onset of the shear or lack thereof.

Two methods of objectively identifying annular hurricanes were developed and discussed in this section. These results, while preliminary, suggest that the identification of annular hurricanes is a possibility in a real-time operational setting using either of these methods. These encouraging results coupled with the intensity forecasting biases occurring with these storms, discussed in section 3b, suggest that future research is needed to determine if the identification of annular hurricanes is useful in improving intensity forecasts.

5. Summary and concluding remarks

The appearance of tropical cyclones in IR imagery differs greatly from case to case and over time. The main focus of this study discusses a category of tropical cyclone, termed annular hurricanes. When annular hurricanes are compared with the greater population of tropical cyclones, as observed in an infrared (IR) data archive of tropical cyclones, they appear distinctly symmetric about their center. Their appearance in IR imagery is characterized by large circular eye features surrounded by a nearly uniform ring of deep convection and a distinct lack of deep convective features (i.e., spiral bands) outside this ring.

During 1995–99 six hurricanes (two Atlantic and four eastern Pacific) were subjectively determined to be annular hurricanes (Fig. 1). It was found that these storms have several features in addition to axisymmetry that separate them from other storms, including systematic formation characteristics, steady intensities, and their existence in only specific environmental conditions.

The evidence presented here suggests that annular hurricane formation is preceded by a dramatic asymmetric mixing event in which possible mesovortices mix eyewall air into the eye and vice versa, as shown in Fig. 4, culminating in the formation of the axisymmetric storms with large eyes (i.e., annular hurricanes). The observed thermodynamic structures of two storms sampled by aircraft (Luis and Dora) as characterized by more uniformly distributed values of θ_e in the eye suggest that a dramatic horizontal mixing event had recently occurred. At the same time the observed wind field suggests that some eye-to-eyewall mixing is still occurring, as shown by the steplike features in the tangential wind that are associated with local vorticity and angular velocity peaks.

Once annular hurricanes have formed, they can maintain their annular shape for days if specific environmental conditions (see Table 4) are maintained. Annular hurricanes are also rather intense, averaging 108 kt, which corresponds to roughly 85% of their MPI with respect to SST. As a result, annular hurricanes pose an interesting challenge when forecasting intensity change. Unlike typical tropical cyclones of hurricane strength, annular hurricanes tend to experience a long period of nearly steady intensities with a relatively slowly decreasing intensity following their maximum intensity as shown in Fig. 3. As a result of this intensity change characteristic, intensity forecast errors are larger for these storms than for the 1995–99 mean, with large negative biases, suggesting that the forecasts overestimate the future rate of filling (see Table 2).

Composite analysis reveals that the typical annular hurricane exists in a very favorable hurricane environment. Such an environment is characterized by the combination of 1) weak easterly or southeasterly vertical wind shear, 2) easterly flow and relatively cold temperatures at 200 hPa, 3) a narrow range (25.4°–28.5°C) of SSTs that are nearly constant, and 4) a lack of 200-hPa relative eddy flux convergence due to environmental interactions (see Tables 3 and 4 for details). These individual characteristics are quite commonly observed, but the combination of these factors is quite rare occurring 0.8% and 3.0% of the time in the Atlantic and eastern Pacific tropical cyclone basins, respectively.

A secondary topic of this paper was the objective identification of annular hurricanes. Two approaches were discussed. The first approach utilizes the digital brightness temperature information contained in the IR imagery. Once azimuthal means of brightness temperature were created, they were normalized to a common size and mean brightness temperature, and then compared to the mean normalized radial brightness temperature profile of annular hurricanes to form an index. The second approach used the environmental conditions to determine whether an annular hurricane could exist. This required that all of the eight factors listed in Table 4 had to be satisfied. Both techniques seem to work well, suggesting that such information could be examined for possible improvements to intensity forecasting.

Although the main purpose of this paper was the documentation of annular hurricanes, several questions about these storms remain. The striking symmetry in IR imagery raises the question, What caused the symmetry? One possibility is the weak and southeasterly vertical wind shear associate with these systems. It has been shown that vertical wind shear leads to systematic asymmetries in vertical motion, precipitation, and convection (Bender 1997; Frank and Ritchie 1999; Willoughby et al. 1984). Annular hurricanes show little evidence of convective asymmetries. Furthermore, Bender's (1997) modeling study shows that vertical wind shear can be caused by the differential advection of planetary vorticity by the baroclinic hurricane vortex. This shear, which is due to the β effect, has similar magnitude but opposite direction to the large-scale environmental vertical shear associated with the annular hurricanes. In this study the environmental wind has

been filtered to remove the storm-scale circulation within 600-km radius but not all of the effects of the β gyres. However, the filtering reduces the magnitude of β gyres by about a factor of 2 for an average-sized hurricane that has β gyres extending to 800–1000 km. Furthermore, even if the storm-scale circulations were not effectively eliminated through this filtering process, the β-gyre-induced vertical wind shear would likely be poorly sampled at the grid spacing (2°–2.5° latitude) of the NCEP analysis data (Franklin et al. 1996). Based upon these observations one could speculate that the environmental vertical wind shear associated with annular hurricanes (weak southeasterly) is compensating for vertical wind shear resulting from tropical cyclone β gyres weakening with height, and thus allowing for greater storm axisymmetry.

Other questions arise from this study that are not so easily answered and that are beyond the scope of this study. Why is there a relative reduction of prominent outer bands? And, why do these storms display slower filling rates than other hurricanes? The observations discussed in this paper simply cannot answer these rather complicated questions. The role of dynamics and thermodynamics in hurricanes and their interwoven nature suggests that these questions as they relate to annular hurricanes are likely better answered by simple diagnostic modeling studies.

In summary, nature produces a nearly symmetric hurricane referred to as annular hurricanes in this study. The documentation of these annular hurricanes shows how they are similar to and different than the general population of tropical cyclones. Using the observations presented here, particularly the environmental conditions associated with these storms, modeling studies specifically designed to focus on the formation and evolutionary characteristics of these storms can be designed and, hopefully, will lead to even greater physical understanding. The differences between annular hurricanes and the greater population of hurricanes have also been used to classify these systems both subjectively and objectively. While the ultimate usefulness of such discrimination is beyond the scope of this study, it does suggest a future research topic answering the question, Does the identification of annular hurricanes lead to better intensity forecasts?

Acknowledgments. The authors thank Kerry Emanuel for supplying his portion of the data for Fig. 3, Wayne Schubert for his very helpful comments, Ray Zehr for continuing to maintain and improve the CIRA/NESDIS tropical cyclone IR archive, and the three anonymous reviewers whose helpful comments greatly improved the manuscript. National Oceanic and Atmospheric Administration Grant NA67RJ0152 supported the research efforts of J. Knaff and J. Kossin.

REFERENCES

Bader, M. J., G. S. Forbes, J. R. Grant, R. B. E. Lilley, and A. J. Waters, 1995: *Images in Weather Forecasting: A Practical Guide for Interpreting Satellite and Radar Imagery*. Cambridge University Press, 499 pp.

Bender, M. A., 1997: The effects of relative flow on asymmetric structures in hurricanes. *J. Atmos. Sci.,* **54,** 703–724.

Davis, M. A. S., G. M. Brown, and P. Leftwich, 1984: A tropical cyclone data tape for the eastern and central North Pacific basins, 1949–1983. NOAA Tech. Memo. NWS NHC **25,** 15 pp.

DeMaria, M., and J. Kaplan, 1994a: A statistical hurricane intensity prediction scheme (SHIPS) for the Atlantic basin. *Wea. Forecasting,* **9,** 209–220.

——, and ——, 1994b: Sea surface temperature and the maximum intensity of Atlantic tropical cyclones. *J. Climate,* **7,** 1324–1334.

——, and ——, 1999: An updated statistical hurricane intensity prediction scheme (SHIPS) for the Atlantic and eastern North Pacific basins. *Wea. Forecasting,* **14,** 326–337.

——, J. Demuth, and J. A. Knaff, 2001: Validation of an Advanced Microwave Sounder Unit (AMSU) tropical cyclone intensity and size estimation algorithm. Preprints, *11th Conf. on Satellite Meteorology and Oceanography,* Madison, WI, Amer. Meteor. Soc., 300–303.

Dvorak, V. F., 1984: Tropical cyclone intensity analysis using satellite data. NOAA Tech. Rep. NESDIS 11, Washington, DC, 47 pp. [Available from National Technical Information Service, 5285 Port Royal Rd., Springfield, VA 22161.]

Eliassen, A., and M. Lystad, 1977: The Ekman layer of a circular vortex: A numerical and theoretical study. *Geophys. Norv.,* **31,** 1–16.

Emanuel, K., 2000: A statistical analysis of tropical cyclone intensity. *Mon. Wea. Rev.,* **128,** 1139–1152.

Frank, W. M., and E. A. Ritchie, 1999: Effects of environmental flow upon tropical cyclone structure. *Mon. Wea. Rev.,* **127,** 2044–2061.

——, and ——, 2001: Effects of vertical wind shear on the intensity and structure of numerically simulated hurricanes. *Mon. Wea. Rev.,* **129,** 2249–2269.

Franklin, J. L., S. E. Feuer, J. Kaplan, and S. D. Aberson, 1996: Tropical cyclone motion and surrounding flow relationships: Searching for beta gyres in Omega dropwindsonde datasets. *Mon. Wea. Rev.,* **124,** 64–84.

Jarvinen, B. R., C. J. Neumann, and M. A. S. Davis, 1984: A tropical cyclone data tape for the North Atlantic basin, 1886–1983: Contents, limitations, and uses. NOAA Tech. Memo. NWS NHC 22, Coral Gables, FL, 21 pp.

Jones, S. C., 1995: The evolution of vortices in a vertical shear. Part I: Initially barotropic vortices. *Quart. J. Roy. Meteor. Soc.,* **121,** 821–851.

Kossin, J. P., 2002: Daily hurricane variability inferred from GOES infrared imagery. *Mon. Wea. Rev.,* **130,** 2260–2270.

——, and M. D. Eastin, 2001: Two distinct regimes in the kinematic and thermodynamic structure of the hurricane eye and eyewall. *J. Atmos. Sci.,* **58,** 1079–1090.

——, and W. H. Schubert, 2001: Mesovortices, polygonal flow patterns, and rapid pressure falls in hurricane-like vortices. *J. Atmos. Sci.,* **58,** 2196–2209.

——, ——, and M. T. Montgomery, 2000: Unstable interactions between a hurricane's primary eyewall and a secondary ring of enhanced vorticity. *J. Atmos. Sci.,* **57,** 3893–3917.

Molinari, J., D. Vollaro, and F. Robasky, 1992: Use of ECMWF operational analyses for studies of the tropical cyclone environment. *Meteor. Atmos. Phys.,* **47** (2–4), 127–144.

Montgomery, M. T., J. M. Hidalgo, and P. D. Reasor, 2000: A semi-spectral numerical method for modeling the vorticity dynamics of the near-core of hurricane-like vortices. Atmospheric Science Paper 695, Dept. of Atmospheric Science, Colorado State University, 56 pp. [Available from Dept. of Atmospheric Science, Colorado State University, Fort Collins, CO 80523.]

——, H. D. Snell, and Z. Yang, 2001: Axisymmetric spindown dynamics of hurricane-like vortices. *J. Atmos. Sci.,* **58,** 421–435.

Reynolds, R. W., and T. M. Smith, 1994: Improved global sea surface

temperature analyses using optimum interpolation. *J. Climate*, **7,** 929–948.

Ritchie, E., and G. J. Holland, 1993: On the interaction of tropical cyclone scale vortices. Part II: Discrete vortex patches. *Quart. J. Roy. Meteor. Soc.*, **119,** 1363–1379.

Schubert, W. H., M. T. Montgomery, R. K. Taft, T. A. Guinn, S. R. Fulton, J. P. Kossin, and J. P. Edwards, 1999: Polygonal eyewalls, asymmetric eye contraction, and potential vorticity mixing in hurricanes. *J. Atmos. Sci.*, **56,** 1197–1223.

Whitney, L. D., and J. S. Hobgood, 1997: The relationship between sea surface temperatures and maximum intensities of tropical cyclones in the eastern North Pacific Ocean. *J. Climate*, **10,** 2921–2930.

Willoughby, H. E., J. A. Clos, and M. G. Shoreibah, 1982: Concentric eye walls, secondary wind maxima, and the evolution of the hurricane vortex. *J. Atmos. Sci.*, **39,** 395–411.

——, F. D. Marks Jr., and R. J. Feinberg, 1984: Stationary and moving convective bands in hurricanes. *J. Atmos. Sci.*, **41,** 3189–3211.

Zehr, R. M., 2000: Tropical cyclone research using large infrared image data sets. Preprints, *24th Conf. on Hurricanes and Tropical Meteorology*, Fort Lauderdale, FL, Amer. Meteor. Soc., 486–487.